Environment International 132 (2019) 105040

Contents lists available at ScienceDirect

Environment International

journal homepage: www.elsevier.com/locate/envint

Rapid determination of the electroporation threshold for bacteria inactivation using a lab-on-a-chip platform

Ting Wang[a], Hang Chen[b], Cecilia Yu[a], Xing Xie[a,*]

[a] School of Civil and Environmental Engineering, Georgia Institute of Technology, Atlanta, GA 30332, United States
[b] Institute for Electronics and Nanotechnology, Georgia Institute of Technology, Atlanta, GA 30332, United States

ARTICLE INFO

Handling Editor: Zhen Jason He

Keywords:
Disinfection
Lethal electroporation threshold (LET)
Lab-on-a-chip
LEEFT
Electric field treatment

ABSTRACT

Electroporation based locally enhanced electric field treatment (LEEFT) is an emerging bacteria inactivation technology for drinking water disinfection. Nevertheless, the lethal electroporation threshold (LET) for bacteria has not been studied, partly due to the tedious work required by traditional experimental methods. Here, a lab-on-a-chip device composed of platinum electrodes deposited on a glass substrate is developed for rapid determination of the LET. When voltage pulses are applied, an electric field with a linear strength gradient is generated on a channel between the electrodes. Bacterial cells exposed to the electric field stronger than the LET are inactivated, while others remain intact. After a cell staining process to differentiate dead and live bacterial cells, the LETs are obtained by analyzing the fluorescence microscopy images. *Staphylococcus epidermidis* has been utilized as a model bacterium in this study. The LETs range from 10 kV/cm to 35 kV/cm under different pulsed electric field conditions, decreasing with the increase of pulse width, effective treatment time, and pulsed electric field frequency. The effects of medium properties on the LET were also investigated. This lab-on-a-chip device and the experimental approach can also be used to determine the LETs for other microorganisms found in drinking water.

1. Introduction and background

Drinking water disinfection is an essential process to guarantee people's access to safe water. The current widely used disinfection method, chlorination, has a major drawback of generating disinfection by-products (DBPs), such as halonitromethanes, which are proved to be cytotoxic and genotoxic (Plewa et al., 2004). Therefore, exploring high-efficiency and environmental-friendly drinking water disinfection approaches is necessary. Electroporation is a technique to create pores on the cell membrane by applying a strong electric field (Tieleman et al., 2003). When the electric field is sufficiently strong, it can also cause cell inactivation (Kotnik et al., 2015). As an efficient method which potentially does not generate DBPs, electroporation was proved to be a promising technique for drinking water disinfection. In several recent studies on locally enhanced electric field treatment (LEEFT), one-dimensional nanomaterial-modified electrodes (e.g., Ag nanowires, CuO nanowires, Cu_3P nanowires, and carbon nanotubes), which can generate extremely high electric field strength near the tip areas of the nanostructures, enabled a 6-log removal efficiency of various bacteria even with a small voltage (1–2 V) (Huo et al., 2017; Huo et al., 2016; Huo et al., 2018b; Liu et al., 2013). Although electroporation is a promising technique, the strong electric field (usually higher than 10 kV/cm) needed for bacteria inactivation makes it a potentially high energy-consuming method, limiting its widespread application (Tian et al., 2017). Therefore, to guarantee the inactivation effect and at the same time reduce the energy consumption, it is essential to find the lethal electroporation threshold (LET), i.e., the lowest electric field strength needed for bacteria inactivation.

When a bacterium is exposed to an external electric field, the cell membrane could be considered as a capacitor in a circuit. Charged ions inside and outside the cell move under electrophoretic force and redistribute on the two sides of the membrane bilayer, generating a transmembrane potential (Kotnik et al., 1997; Tsong, 1989). Under this potential, water molecules tend to penetrate across the lipid bilayer, leading to a reorientation of lipids with their heads towards water molecules and initiating the generation of aqueous pores (Sengel and Wallace, 2016). When the transmembrane potential is not sufficiently high, the pores are transient and could reseal after the electric field is removed. This phenomenon is called reversible electroporation, which has been widely used for drug or DNA delivery (Alvarez-Erviti et al., 2011). If the voltage reaches a threshold where the pores become permanent, then irreversible electroporation happens, causing cell

* Corresponding author.
E-mail address: xing.xie@ce.gatech.edu (X. Xie).

https://doi.org/10.1016/j.envint.2019.105040
Received 19 April 2019; Received in revised form 4 July 2019; Accepted 19 July 2019
Available online 03 August 2019

inactivation. Also, although pores formed during reversible electroporation are resealable, they may cause cell death, since the resealing process might be long, and cytoplasm leakage and toxic compound uptake may take place (Jiang et al., 2015). In the present study, we aimed to find the lowest electric field strength that causes cell inactivation without differentiating if the electroporation is reversible or irreversible.

The typical in vitro electroporation was carried out in a cuvette with parallel plane electrodes (Stewart et al., 2018). The cell suspension was first treated under a certain electric field strength, and then the cell inactivation efficiency was tested by microbial culturing. Nevertheless, to determine the LET, a series of different electric field strength should be tested. Such a tedious process greatly hindered the investigation of the LET. To the best of our knowledge, no systematic LET data for microorganisms have been reported. Therefore, a more rapid and efficient method is necessary. A lab-on-a-chip device is a powerful tool for electroporation since it overcomes several disadvantages of bulk electroporators (Boukany et al., 2011). With the much smaller distance between electrodes, which is usually tens of micrometers, it is capable of generating a higher electric field with significantly lower voltage. Several studies have been conducted to implement electroporation on lab-on-a-chip devices, including electroporation of mammalian cells using a carbon nanotube-featured microfluidics chip (Shahini and Yeow, 2013), synthesizing erythrocyte membrane-coated magnetic nanoparticles by electroporation (Rao et al., 2017), and selectively lysing cells with different shapes on a optoelectronic platform (Kremer et al., 2014). Lab-on-a-chip devices have also been utilized for electroporation mechanism study, since they enabled the precise control of electroporation parameters and in situ observation of the process (Geng and Lu, 2013). The intracellular effect of nanosecond electrical pulses has been investigated with a removable packaging microfluidic chip (Dalmay et al., 2012). The reversible electroporation threshold, rather than the LET, of several kinds of bacteria has been studied in a microfluidic device (Garcia et al., 2016).

Here, we report a lab-on-a-chip platform to rapidly determine the LET of bacteria. The proposed approach for the LET determination is illustrated in Fig. 1: i) bacterial cells are immobilized onto a glass substrate and exposed to an electric field with linear strength gradient; ii) the cells exposed to the electric field stronger than the LET will be inactivated, while the others are still intact; and iii) the LET could be determined by combining live/dead cell staining and image processing methods. Through such an approach, the LETs of a model bacterial strain, *Staphylococcus epidermidis*, under different pulsed electric field treatment conditions have been investigated and are reported for the first time in this study. Effects of different media properties, including conductivity, temperature, pH, and disinfection ions, have also been studied.

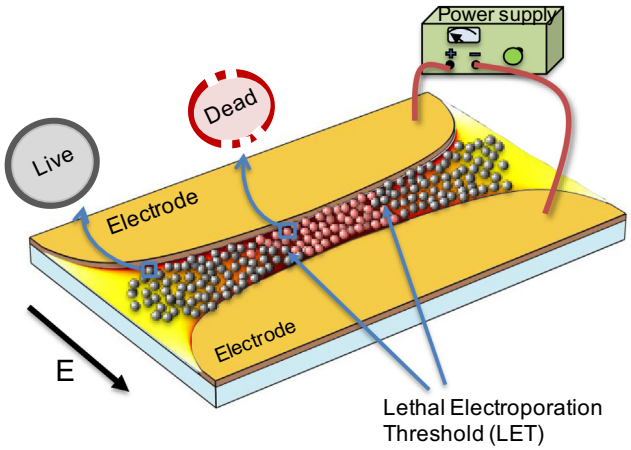

Fig. 1. Schematic illustration of the lab-on-a-chip platform for the lethal electroporation threshold (LET) determination. The red and gray spheres represent inactivated and live bacteria, respectively. The color underneath the cells between two electrodes represents the strength of the electric field. Darker red indicates higher electric field strength. (For interpretation of the references to color in this figure legend, the reader is referred to the web version of this article.)

2. Materials and methods

2.1. Fabrication of the lab-on-a-chip device

The lab-on-a-chip device was constructed by depositing platinum electrodes on a glass substrate. Photolithography and lift-off methods were used for the fabrication (Fig. 2a). Specifically, a layer of negative photoresist NR9-1500py was spin-coated onto the surface of a Borofloat 33 glass wafer; then, the coated wafer was exposed to UV light using a maskless aligner, and the pattern was developed by a developer solution. Titanium (10 nm thick) and platinum (100 nm thick) were subsequently deposited onto the surface by the e-beam evaporation method, where the Ti layer served as an attachment layer (Chung et al., 2015). After deposition, the residual photoresist was removed with acetone, leaving the metal electrodes on the chip surface.

2.2. Cell preparation

Staphylococcus epidermidis (*S. epidermidis*) (ATCC 12228) was used as a model bacterial strain to quantitatively determine the LET. It is a commonly used bacterial strain for water disinfection and antimicrobial tests (Helbling and VanBriesen, 2007; Wen et al., 2017). The bacteria solution was prepared as follows: *S. epidermidis* was incubated in nutrient broth at 35 °C till stationary phase (15 h); 1 mL of cells was centrifuged at 5000 rpm for 5 min and resuspended in 10 mM phosphate buffer for three times; the washed cells were resuspended to 1 mL with 10 mM phosphate buffered solution to obtain the experimental bacterial solution.

2.3. Electric field treatment

The lab-on-a-chip device was pre-treated with poly-L-lysine, which coated the chip surface with positive charges to immobilize the negatively charged bacteria cells on the channel between the two electrodes. Specifically, poly-L-lysine (Sigma, molecular weight 150,000-300,000, 0.01%) was dropped onto the chip surface and let rest for 2 h, then rinsed with deionized (DI) water and dried in 60 °C for 30 min. The prepared bacteria solution was dropped onto the chip and let rest for 40 min to allow cell attachment. Then, the chip surface was gently rinsed with DI water to remove the unattached bacteria, leaving the attached bacteria immersed in a droplet of DI water. Subsequently, square-wave pulsed voltage shocks (typically 100 V) with different parameters, including pulse width (1–50 μs), frequency (1–50 kHz), and effective time, which is the product of pulse width and pulse number (10^3–10^6 μs) (Fig. S1), were applied to the lab-on-a-chip device using a high-speed pulse generator (Avtech AV-1010-B) triggered with a waveform generator (Keysight 33509B).

The effects of medium properties, including conductivity, temperature, pH, and Cu^{2+} concentration, were investigated. Media with conductivities ranging from 5×10^{-5} S/m to 1 S/m were prepared with $Na_2S_2O_3$ as solute to eliminate the effect of possible electrochemical reactions (Hülsheger et al., 1981). The pulse width and frequency were fixed at 1 μs and 10 kHz, respectively, while two effective times, 10^3 and 10^4 μs, were tested. Temperature control of the experiments in the range of 4 to 45 °C was realized by putting the samples in an incubator at different temperatures. The 10 mM phophate buffer medium pH ranging from 4.5 to 12 was adjusted by NaOH (0.1 M) and HCl (0.1 M). Media with different Cu^{2+} concentration (0–800 μg/L) were achieved by adding $CuSO_4$. For the assays on the impact of temperature, pH, and

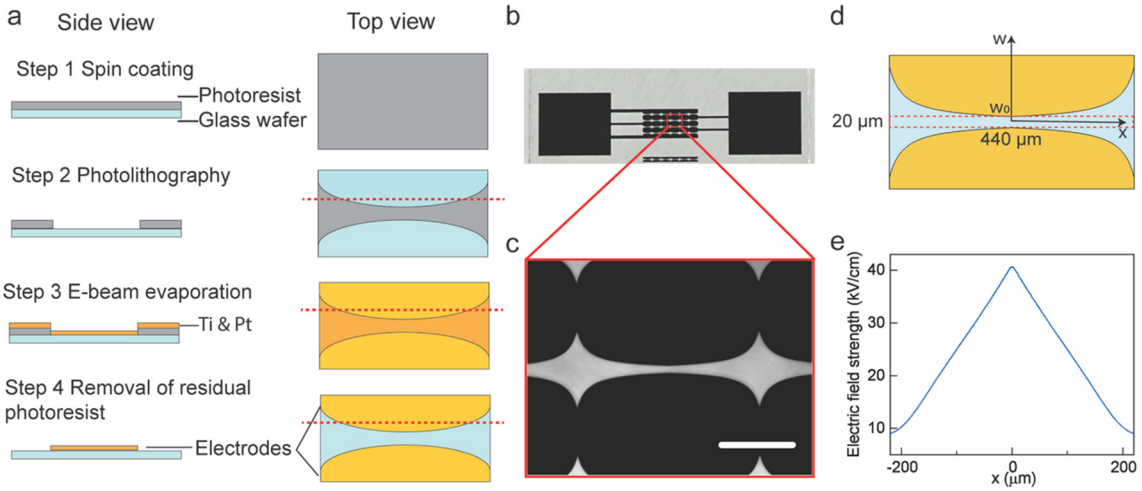

Fig. 2. Design and fabrication of the lab-on-a-chip device. (a) Fabrication procedure with both side view and top view. The side view is drawn across the red dashed line in the top view images. (b, c) A digital photo of the lab-on-a-chip device and a zoom-in microscopy image of the channel. The scale bar is 200 μm. (d) Design of the electrodes. The curving edge of the electrode is designed according to Eq. (1) in the x-w coordinate. The red dashed frame indicates the rectangular area selected for data analysis. (e) Electric field distribution in the channel simulated with COMSOL Multiphysics when 100 V is applied. (For interpretation of the references to color in this figure legend, the reader is referred to the web version of this article.)

Cu^{2+}, the applied pulse width, frequency, and effective time were fixed at 1 μs, 10 kHz, and 10^3 μs, respectively.

2.4. Imaging and data processing

Cell viability was tested by Propidium Iodide (PI) staining, since PI molecules only enter dead bacteria with a compromised membrane, and bind to DNA and show a fluorescence enhanced 20 to 30 folds. Some of the bacteria with intact cell membranes may enter the viable but non culturable state after antimicrobial treatment, but they are still potentially risky (Robben et al., 2018). Thus, we tested the membrane integrity in this study to guarantee the inactivation status of bacteria. After electroporation treatment, the treated bacteria were immersed in a droplet of 10 mM phosphate buffer for 1.5 h to reach a stable cell condition, i.e., live or dead. Then, the bacteria were stained with 3 μM Propidium Iodide (PI) solution and incubated for 30 min protected from light. Microscopy images of differential interference contrast (DIC) and fluorescent channel were taken using a Zeiss inverted fluorescent microscope (Axio observer 7) connected to a CCD camera. The images were processed with MATLAB (see the MATLAB code and explanation in Supplementary information (SI) Section 4). Briefly, a rectangular part of the channel, which is 440 μm long and 20 μm high, was cropped in each image, and then vertically divided into 120 columns, and the cell number in each column was counted. The inactivation efficiency in each column was calculated by dividing the number of inactivated cells (from fluorescent image) by the number of total cells (from DIC image) in the same column. The electric field strength causing 50% cell inactivation was found, and the results from parallel channels on one chip were used collectively to determine the LET.

3. Results and discussion

3.1. The lab-on-a-chip device

A digital photo of the fabricated lab-on-a-chip device and a zoom-in microscopy image of the channel are shown in Fig. 2b and c. A total of 4 × 6 channel units were fabricated on one chip for parallel experiments. The curving edge of the symmetric electrode was designed according to Eq. (1) in the coordinate in Fig. 2d:

$$w = \frac{w_0}{1 + kx} \quad (1)$$

where x and w represent the half length and width of the channel, w_0 is the half width at $x = 0$, and k is a constant (Garcia et al., 2016; Weiss et al., 2011). As shown in Fig. 2d, the length of the channel unit is 440 μm, and the narrowest width at the center is 20 μm. The electric field strength can be calculated by the equation $E = V/(2w)$, where E is the electric field, and $2w$ is the distance between the two electrodes. Because of the shape of the electrode edge, when a certain voltage is applied to the two electrodes, an electric field with a linear strength gradient will be generated in the channel. This electric field strength was simulated by COMSOL Multiphysics in a 3D model (Fig. 2e), considering the 3D geometry effect. When a voltage of 100 V is applied, the electric field strength reaches about 40 kV/cm (see the specific simulation method in SI Section 1.1).

3.2. The LET

Fig. 3a shows a DIC image and a fluorescent image stacked together, both taken at the same position after an electric field treatment. The applied pulse voltage is 100 V, the pulse width is 1 μs, frequency is 4 kHz, and the effective time is 10^4 μs. The DIC image shows that bacterial cells are uniformly distributed on the channel (Fig. 3b), while the red dots in the fluorescent image represent dead cells stained by PI (Fig. 3c). It is evident that only the bacteria distributed in the middle section of the channel are stained with PI, indicating that these bacteria have been exposed to the electric field stronger than the LET and have been inactivated. The inactivation efficiencies along the channel are plotted in Fig. 3d. The regression line (least square fitting) indicates that the inactivation efficiency increases from lower than 5% to about 100% within a narrow range. The positions (x values) showing 50% inactivation are about ± 72 μm (Fig. 3d). Subsequently, the corresponding electric field strength at this position is determined to be 29.16 kV/cm, based on the electric field distribution along the channel (Fig. 3e). Finally, the LET of *S. epidermidis* under such electroporation treatment condition is reported to be 29.50 ± 0.16 kV/cm after averaging the parallel results from 24 channel units on one chip.

3.3. LETs under different pulsed electric field conditions

The LET is collectively determined by several parameters of the pulsed electric field, including pulse width (λ), frequency (f) and effective time (t) (Fig. S1). Under the treatment conditions listed in Fig. 4, the LETs range between 10 kV/cm to 35 kV/cm. The error bars

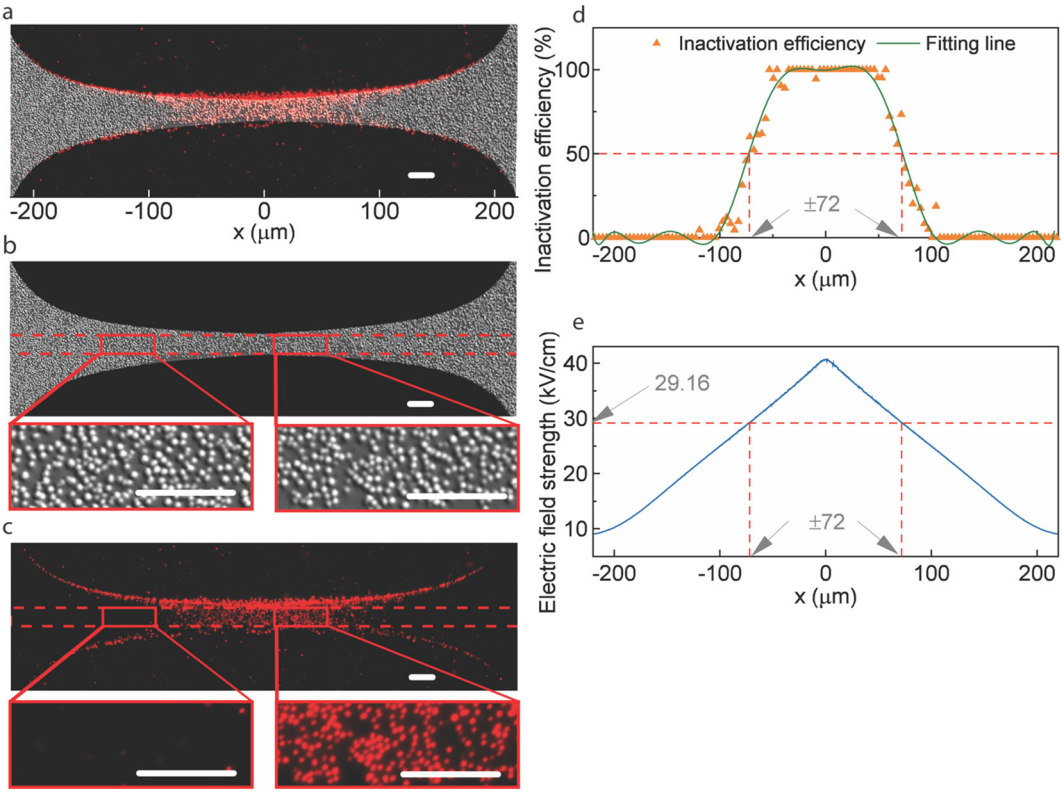

Fig. 3. An example of microscopy images and data processing method (pulse width, 1 μs; frequency, 4 kHz; effective time, 10^4 μs; and applied voltage, 100 V). (a) A stacked image of a DIC and a fluorescent microscopy image. (b) A DIC image and zoom-in images showing all bacteria attached on the substrate in the channel. The dashed frame represents the area selected for data analysis. (c) A fluorescent image and zoom-in images of bacteria stained by propidium iodide (PI). (d) Inactivation efficiency and the fitted line plotted along the length of the channel. The value " ± 72" on the x-axis represents the locations where the inactivation efficiency is 50%. (e) Electric field strength along the length of the channel. The value "29.16" on the y-axis represents the corresponding electric field strength at the defined locations. The scale bars are 20 μm for all microscopy images.

represent 95% confidence intervals. The previously reported electroporation thresholds for mammal cells were mostly distributed between 0.5 and 2 kV/cm (Henslee et al., 2011; Jiang et al., 2015). The reversible electroporation thresholds for bacteria were found to be 3–6 kV/cm, which should be lower than their irreversible threshold (Garcia et al., 2016). Other studies also stated that irreversible electroporation often requires an electric field strength greater than 10 kV/cm (Tian et al., 2017).

At a fixed pulse width and frequency (individual lines in Fig. 4a), a negative correlation between the LET and effective time can be observed. This correlation is intuitive: being exposed to an electric field for a longer time generates more and larger pores on the cell membrane, thus, lower electric field strength is needed for bacteria inactivation. The electroporation threshold on synthetic lipid bilayers showed a similar trend, except that the threshold decreased linearly with the logarithmic increase of the effective time (Troiano et al., 1998). In the present study, the LET decreases significantly in most cases when the effective time increase from 10^2 to 10^3 μs, then slows down when further increasing the effective time. This might be attributed to the recovery ability of the cell membrane, which is lacking for artificial membranes. This recovery ability may be stronger when cells are exposed to a weaker electric field. Thus, longer effective treatment time is required to achieve lethal electroporation.

The electroporation process under pulsed electric field could be

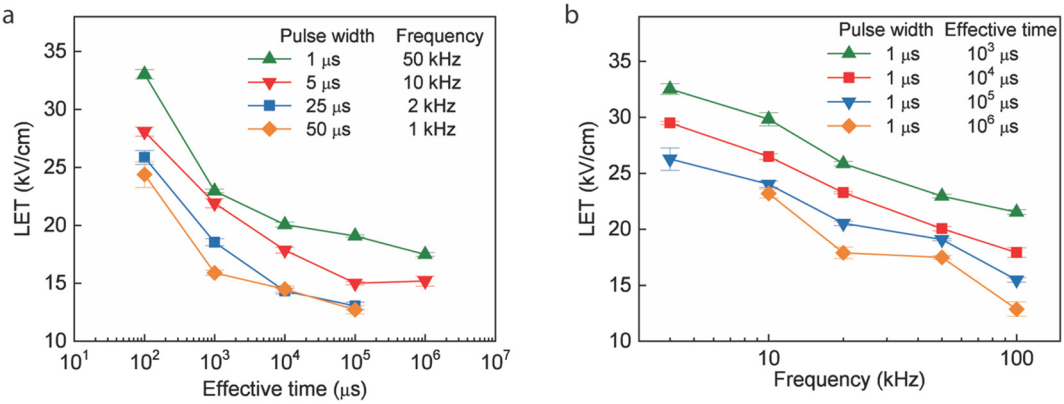

Fig. 4. The LETs of *S. epidermidis* under different pulsed electric field conditions. (a) Dependence of the LET on effective time at different pulse widths and frequencies (with the same pulse width to period ratio). (b) Relationship between the LET and frequency at the same pulse width but different effective times.

considered as a series of repeated pore-forming and closing processes. When a strong electrical pulse is applied, pores form on the membrane and compounds on the two sides start to exchange through the pores. When the electric field is removed between two pulses, the cell membrane may reseal during this interval (Sengel and Wallace, 2016). The four lines in Fig. 4a represent the LETs at different pulse width and frequency, but the ratios of pulse width to period ($T = 1/f$) are all 1:20, which means that a longer pulse is followed by a longer resting time for the pores to close. Thus, the total treatment times (including the resting time) are the same for the four lines when they have the same effective times. The difference between the four lines (Fig. 4a) indicates that increasing the width of each pulse is effective in reducing the LET even though a longer interval is provided for the membrane to recover. With a longer pulse width, the pores may have already grown to the size or phase that cannot be easily closed, no matter how long the interval that follows. In addition, the larger pores generated may allow more compounds to exchange across the membrane, causing greater or irreversible damage. Nevertheless, in real applications, a trade-off needs to be considered for applying longer pulse widths, since it may cause electrochemical reactions that waste the energy on water splitting.

Fig. 4b shows the negative correlation between the LET and the frequency of the pulsed electric field when the pulse width is fixed at 1 μs. For the same pulse width, a higher frequency means a shorter interval between two pulses, so that the membrane may not have enough time to fully recover during the interval. Therefore, the pores keep growing when a new pulse is applied, increasing the probability of membrane rupture and cell death, and thus decreasing the LET. The same trend is observed for various effective times in this study, and has also been reported in a previous study on artificial lipid bilayers (Lebar et al., 2002).

3.4. Effects of medium properties on LET

Different properties of drinking water, such as the conductivity, pH value, temperature, and ion species, may all affect the LET of bacteria. Thus, the effects of these medium properties have been investigated with the developed platform.

3.4.1. Conductivity

During electric field treatment, charging the cell membrane can be considered as charging a capacitor in a circuit (Tsong, 1989), and the extracellular medium acts as a resistor in the circuit. Therefore, the conductivity of the extracellular medium will affect the transmembrane potential and the LET. Fig. 5a shows the changing of the LET with the medium conductivity. The range of the conductivities tested (5×10^{-5} to 1 S/m) covers the values of typical environmental water samples. Results from the experiments with two different effective times (10^3 and 10^4 μs) show a similar trend: the LET decreases with the increase of medium conductivity, especially in the range of 2×10^{-3} to 0.1 S/m. Based on the theoretical model (see the additional discussion in SI Section 2), the electric field strength required to achieve the same level of transmembrane potential (e.g., 1 V) at different medium conductivities can be calculated. The results of the theoretical calculations (Fig. S2) and our experiment (Fig. 5a) showed a similar trend.

3.4.2. Temperature

Temperature may change the fluidity and permeability of the bacteria membrane, thus affecting the LET (Denich et al., 2003). To investigate the temperature effects, bacteria were electric field-treated at 4 °C, 45 °C, and room temperature (23 °C), respectively. The results are depicted in Fig. 5b, where the red dots represent the LETs when the bacteria were put into 4 °C or 45 °C and directly subjected to the electric field treatment, while for the green dots, the bacteria were first put into the corresponding temperatures for pre-heating or cooling for 40 min, and then treated with electric field. The LET at 45 °C is slightly lower than that at room temperature without pre-treatment (red squares). According to a previous study, *Staphylococcus* became more sensitive to pulsed electric field treatment with the increase of treatment temperature (Cebrián et al., 2016). It might be due to the reduction of the membrane charging time, or the decrease of the minimum transmembrane potential needed to disrupt the cell membrane at a higher temperature (Coster and Zimmermann, 1975; Schwan, 1957). When the bacteria were pre-cooled or heated, the LETs both slightly increased (green squares compared to red squares). It was reported that heat-pretreated cells tended to have higher heat resistance and damage repair capability, which could mitigate the adverse effect of high treatment temperature (Parsell and Lindquist, 1993). An increase of electroporation resistance was also observed in a previous study when *Escherichiacoli* (*E. coli*) was treated with previous cold shock (Somolinos et al., 2008).

3.4.3. pH

An important parameter affecting biological systems, pH should also be considered. Extreme pH may interfere with the bacteria membrane reseal-capability and inactive the injured bacteria, thus decreasing the LET (Somolinos et al., 2008). To test these effects, bacteria have been first treated in DI water and then immersed in media with different pH. Within a pH range of 4.5 to 12, the LET was only affected slightly between 28.6 and 32.1 kV/cm (Fig. 5c). A previous study demonstrated that after a post-storage in citrate-phosphate buffer of pH 4.0 for 4 h, the inactivation efficiency of *E. coli* by electroporation increased significantly. This indicated that the sublethal injured bacteria might be sensitive to low pH conditions (Somolinos et al., 2008). The same outcome has not been found in the present study, which might be due to the slightly higher pH (4.5 compared with 4.0), shorter post-storage time (1.5 h compared with 4 h), or the different properties between *S. epidermidis* and *E. coli*. Nevertheless, results of our previous study on LEEFT indicated that pH ranging from 3 to 11 did not affect the disinfection efficiencies of *E. coli* (Huo et al., 2018a). The mechanism of pH influence is still not clear and needs further study.

3.4.4. Copper (II) ions (Cu^{2+})

Using antimicrobial metal ions, such as Cu^{2+} or Ag^{+}, is another efficient water disinfection technique (Chen et al., 2019; Hajipour et al., 2012). Electroporation may work synergistically with these metal ions since the formation of transient pores and increase of membrane permeability may assist the delivery of microbiocidal ions into the cells (Zhou et al., 2019). If such synergistic effect exists, the LETs will be lower. The effect of Cu^{2+} on the LET is depicted in Fig. 5d. The blue dots show the LETs when Cu^{2+} is only present during the electric field treatment process (~5 s including some handling processes), while the red dots represent the results when Cu^{2+} is present both during and after treatment for 1.5 h. A slight decrease of the LET with the increase of Cu^{2+} concentration is noted for the red line, which indicates that higher Cu^{2+} concentration in the medium may reduce the LET. Nevertheless, the blue line shows little change, indicating that the extra Cu^{2+} uptake only during the electric field treatment does not cause significant antimicrobial effect. Collectively, the results suggest that microbiocidal ions in the medium may decrease the LET, but sufficient time is required for the ions to transport into the cells.

4. Perspective

From the threshold values we measured, the energy consumption for bacteria inactivation could be further investigated. The energy consumption of the electric field treatment process is determined by both the strength and duration of the applied electric field. In this study, we define the product of the LET and effective time as the energy index to represent the energy consumption required for bacteria inactivation. Comparable to the “CT” value (the product of concentration of a disinfectant, C, and the contact time with water, T), which represents disinfectant dosage in water chlorination, the energy index can

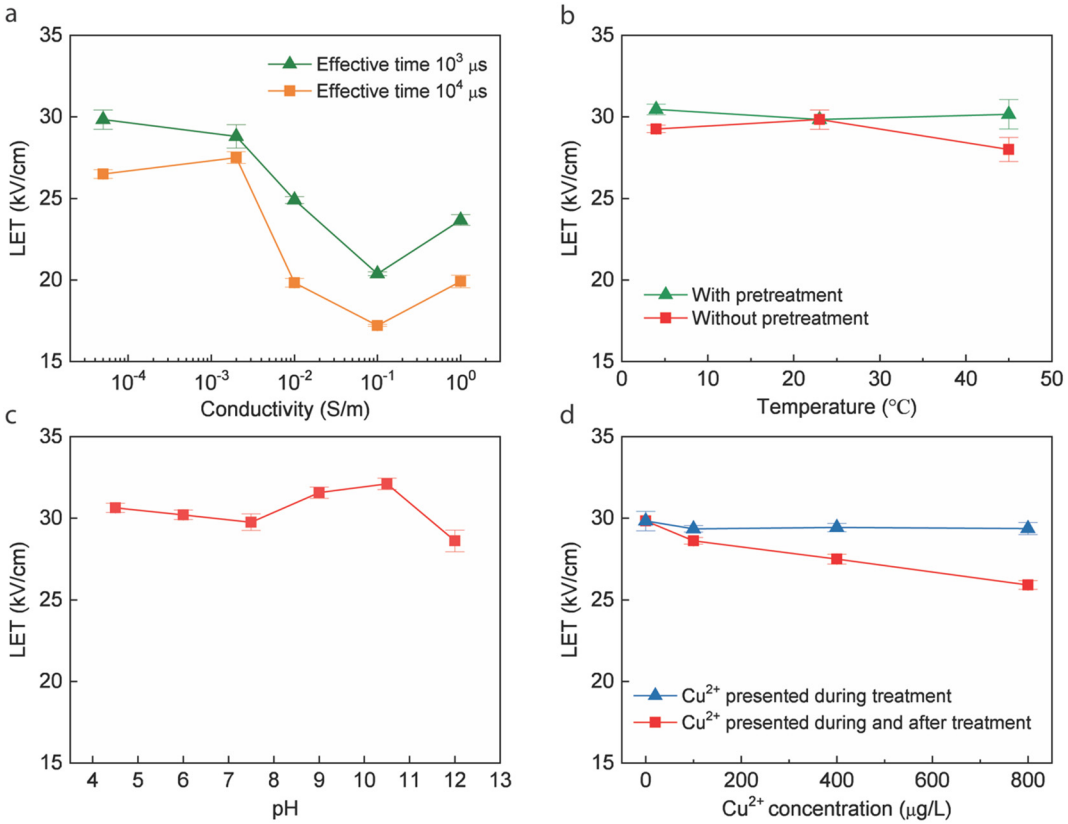

Fig. 5. Effects of medium properties on the LET. (a) Effects of medium conductivity on the LET. The pulse width is 1 μs and frequency is 10 kHz. (b–d) Effects of temperature, pH, and Cu^{2+} concentration of medium on the LET. The pulse width is 1 μs, frequency is 10 kHz, and effective time is 10^3 μs. (For interpretation of the references to color in this figure, the reader is referred to the web version of this article.)

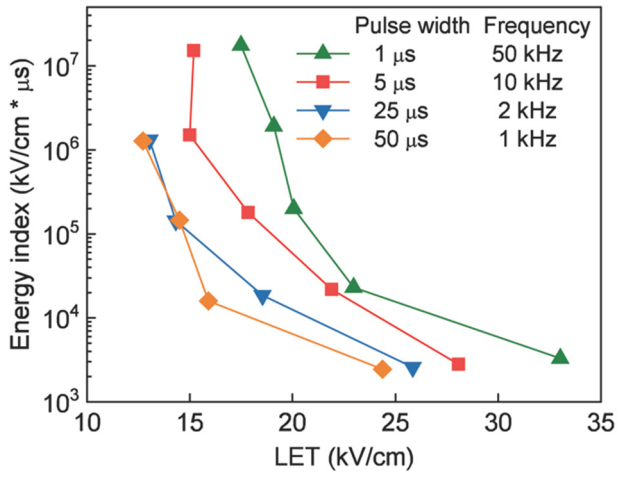

Fig. 6. Changing of the energy index (the product of the LET and effective time) with the LET.

provide guidance for the electric field treatment system's design (Crittenden et al., 2012). As shown in Fig. 6, the energy index decreases with the increase of the LET, indicating that the energy consumption will be lower if a higher electric field can be applied. This trend could be explained by the much shorter effective time needed for bacterial inactivation when a stronger electric field is applied. This result also indicates the importance of electric field strength for electric field treatment disinfection. To achieve the same disinfection effect, when a stronger electric field is applied, the process could become not only more time efficient, but also more energy efficient. However, there is a trade-off of providing a strong electric field, since it has a risk of causing safety issues, such as arc discharge. The trend of the four lines of different pulse width in Fig. 6 also suggests that longer pulse width is preferred for saving energy. Nevertheless, the same trade-off has to be considered. Based on our previous study, a low energy consumption was achieved with LEEFT disinfection process, which was 1.2 J per litter of water (Huo et al., 2018b). The energy consumption trend found in the present work could be used to further optimize the treatment process and reduce the energy consumption.

Investigating the LET of various pathogens is of great significance for implementing LEEFT technology in water disinfection. The development of the lab-on-a-chip platform here makes it more convenient and rapid to determine the LET. According to the LET values and changing trends, the treatment parameters of the LEEFT process could be more rationally designed, which helps guarantee the disinfection efficiency as well as reduce energy consumption. For the future studies, this platform will be applied to study the LET of other bacterial strains and potentially protozoa. Other impact factors, such as different organics in water, growth status and membrane structures of bacteria could also be studied. In the meantime, the lab-on-a-chip device will be further improved by combining pre-treatment, sample loading, electric field treatment, post-treatment storage, and cell staining into one device.

5. Conclusion

In summary, we have developed a platform combining a lab-on-a-chip device, live/dead cell staining, and image processing methods to rapidly and quantitatively study the LET for bacteria. The LETs of *Staphylococcus* ranged from 10 to 35 kV/cm when the applied pulsed electric field had pulse widths of 1 to 50 μs, frequencies of 4 to 100 kHz, and effective treatment times of 1 ms to 1 s. Decrease of the LET was

noted when a higher effective time, a longer pulse width, or a higher pulse frequency was applied. With higher conductivity, the LET was lower. The presence of Cu^{2+} in the medium may also reduce the LET, while the effects of temperature and pH were not significant in the present study.

Declaration of Competing Interest

The authors declare no competing financial interest.

Acknowledgements

This work was supported by the National Science Foundation [grant numbers CBET 1845354]. This work was performed in part at the Georgia Tech Institute for Electronics and Nanotechnology, a member of the National Nanotechnology Coordinated Infrastructure (NNCI), which is supported by the National Science Foundation [grant numbers ECCS-1542174]. The authors would like to thank Guanxuan Zhu for his help on experimental set-ups and lab safety management. T.W. is grateful for the financial support provided by the China Scholarship Council.

Appendix A. Supplementary data

Supplementary data to this article can be found online at https://doi.org/10.1016/j.envint.2019.105040.

References

Alvarez-Erviti, L., Seow, Y., Yin, H., Betts, C., Lakhal, S., Wood, M.J., 2011. Delivery of siRNA to the mouse brain by systemic injection of targeted exosomes. Nat. Biotechnol. 29, 341.
Boukany, P.E., Morss, A., Liao, W., Henslee, B., Jung, H., Zhang, X., Yu, B., Wang, X., Wu, Y., Li, L., 2011. Nanochannel electroporation delivers precise amounts of biomolecules into living cells. Nat. Nanotechnol. 6, 747.
Cebrián, G., Condón, S., Mañas, P., 2016. Influence of growth and treatment temperature on Staphylococcus aureus resistance to pulsed electric fields: relationship with membrane fluidity. Innovative Food Sci. Emerg. Technol. 37, 161–169.
Chen, W., Jiang, J., Zhang, W., Zhou, J., Wang, T., Huang, C.-H., Xie, X., 2019. Silver nanowire-modified filter with controllable silver ion release for point-of-use disinfection. Environ. Sci. Technol. 53, 7504–7512.
Chung, Y.-C., Chen, Y.-S., Lin, S.-H., 2015. Enhancement for gene transfection of low-descent-velocity bacteria using magnetic attraction in electroporation chip. Sensors Actuators B Chem. 213, 261–267.
Coster, H.G., Zimmermann, U., 1975. The mechanism of electrical breakdown in the membranes of Valonia utricularis. J. Membr. Biol. 22, 73–90.
Crittenden, J.C., Trussell, R.R., Hand, D.W., Howe, K.J., Tchobanoglous, G., 2012. MWH's Water Treatment: Principles and Design. edˆeds. John Wiley & Sons.
Dalmay, C., De Menorval, M., Francais, O., Mir, L., Le Pioufle, B., 2012. A microfluidic device with removable packaging for the real time visualisation of intracellular effects of nanosecond electrical pulses on adherent cells. Lab Chip 12, 4709–4715.
Denich, T., Beaudette, L., Lee, H., Trevors, J., 2003. Effect of selected environmental and physico-chemical factors on bacterial cytoplasmic membranes. J. Microbiol. Methods 52, 149–182.
Garcia, P.A., Ge, Z., Moran, J.L., Buie, C.R., 2016. Microfluidic screening of electric fields for electroporation. Sci. Rep. 6, 21238.
Geng, T., Lu, C., 2013. Microfluidic electroporation for cellular analysis and delivery. Lab Chip 13, 3803–3821.
Hajipour, M.J., Fromm, K.M., Ashkarran, A.A., de Aberasturi, D.J., de Larramendi, I.R., Rojo, T., Serpooshan, V., Parak, W.J., Mahmoudi, M., 2012. Antibacterial properties of nanoparticles. Trends Biotechnol. 30, 499–511.
Helbling, D.E., VanBriesen, J.M., 2007. Free chlorine demand and cell survival of microbial suspensions. Water Res. 41, 4424–4434.
Henslee, B.E., Morss, A., Hu, X., Lafyatis, G.P., Lee, L.J., 2011. Electroporation dependence on cell size: optical tweezers study. Anal. Chem. 83, 3998–4003.
Hülsheger, H., Potel, J., Niemann, E.-G., 1981. Killing of bacteria with electric pulses of high field strength. Radiat. Environ. Biophys. 20, 53–65.
Huo, Z.-Y., Xie, X., Yu, T., Lu, Y., Feng, C., Hu, H.-Y., 2016. Nanowire-modified three-dimensional electrode enabling low-voltage electroporation for water disinfection. Environ. Sci. Technol. 50, 7641–7649.
Huo, Z.-Y., Luo, Y., Xie, X., Feng, C., Jiang, K., Wang, J., Hu, H.-Y., 2017. Carbon-nanotube sponges enabling highly efficient and reliable cell inactivation by low-voltage electroporation. Environ. Sci. Nano 4, 2010–2017.
Huo, Z.-Y., Li, G.-Q., Yu, T., Lu, Y., Sun, H., Wu, Y.-H., Yu, C., Xie, X., Hu, H.-Y., 2018a. Impact of water quality parameters on bacteria inactivation by low-voltage electroporation: mechanism and control. Environ. Sci.: Water Res. Technol. 4, 872–881.
Huo, Z.-Y., Zhou, J.-F., Wu, Y., Wu, Y.-H., Liu, H., Liu, N., Hu, H.-Y., Xie, X., 2018b. A Cu 3 P nanowire enabling high-efficiency, reliable, and energy-efficient low-voltage electroporation-inactivation of pathogens in water. J. Mater. Chem. A 6, 18813–18820.
Jiang, C., Davalos, R.V., Bischof, J.C., 2015. A review of basic to clinical studies of irreversible electroporation therapy. IEEE Trans. Biomed. Eng. 62, 4–20.
Kotnik, T., Bobanović, F., Miklavc˘Ic˘, D., 1997. Sensitivity of transmembrane voltage induced by applied electric fields—a theoretical analysis. Bioelectrochemistry 43, 285–291.
Kotnik, T., Frey, W., Sack, M., Meglič, S.H., Peterka, M., Miklavčič, D., 2015. Electroporation-based applications in biotechnology. Trends Biotechnol. 33, 480–488.
Kremer, C., Witte, C., Neale, S.L., Reboud, J., Barrett, M.P., Cooper, J.M., 2014. Shape-dependent optoelectronic cell lysis. Angew. Chem. 126, 861–865.
Lebar, A.M., Troiano, G.C., Tung, L., Miklavcic, D., 2002. Inter-pulse interval between rectangular voltage pulses affects electroporation threshold of artificial lipid bilayers. IEEE Trans. Nanobioscience 99, 116–120.
Liu, C., Xie, X., Zhao, W., Liu, N., Maraccini, P.A., Sassoubre, L.M., Boehm, A.B., Cui, Y., 2013. Conducting nanosponge electroporation for affordable and high-efficiency disinfection of bacteria and viruses in water. Nano Lett. 13, 4288–4293.
Parsell, D., Lindquist, S., 1993. The function of heat-shock proteins in stress tolerance: degradation and reactivation of damaged proteins. Annu. Rev. Genet. 27, 437–496.
Plewa, M.J., Wagner, E.D., Jazwierska, P., Richardson, S.D., Chen, P.H., McKague, A.B., 2004. Halonitromethane drinking water disinfection byproducts: chemical characterization and mammalian cell cytotoxicity and genotoxicity. Environ. Sci. Technol. 38, 62–68.
Rao, L., Cai, B., Bu, L.-L., Liao, Q.-Q., Guo, S.-S., Zhao, X.-Z., Dong, W.-F., Liu, W., 2017. Microfluidic electroporation-facilitated synthesis of erythrocyte membrane-coated magnetic nanoparticles for enhanced imaging-guided cancer therapy. ACS Nano 11, 3496–3505.
Robben, C., Fister, S., Witte, A.K., Schoder, D., Rossmanith, P., Mester, P., 2018. Induction of the viable but non-culturable state in bacterial pathogens by household cleaners and inorganic salts. Sci. Rep. 8, 15132.
Schwan, H.P., 1957. Electrical properties of tissue and cell suspensions. In: Advances in Biological and Medical Physics. Elsevier.
Sengel, J.T., Wallace, M.I., 2016. Imaging the dynamics of individual electropores. Proc. Natl. Acad. Sci. U. S. A. 113, 5281–5286.
Shahini, M., Yeow, J.T., 2013. Cell electroporation by CNT-featured microfluidic chip. Lab Chip 13, 2585–2590.
Somolinos, M., García, D., Mañas, P., Condón, S., Pagán, R., 2008. Effect of environmental factors and cell physiological state on Pulsed Electric Fields resistance and repair capacity of various strains of Escherichia coli. Int. J. Food Microbiol. 124, 260–267.
Stewart, M.P., Langer, R., Jensen, K.F., 2018. Intracellular delivery by membrane disruption: mechanisms, strategies, and concepts. Chem. Rev. 118, 7409–7531.
Tian, J., Feng, H., Yan, L., Yu, M., Ouyang, H., Li, H., Jiang, W., Jin, Y., Zhu, G., Li, Z., 2017. A self-powered sterilization system with both instant and sustainable antibacterial ability. Nano Energy 36, 241–249.
Tieleman, D.P., Leontiadou, H., Mark, A.E., Marrink, S.-J., 2003. Simulation of pore formation in lipid bilayers by mechanical stress and electric fields. J. Am. Chem. Soc. 125, 6382–6383.
Troiano, G.C., Tung, L., Sharma, V., Stebe, K.J., 1998. The reduction in electroporation voltages by the addition of a surfactant to planar lipid bilayers. Biophys. J. 75, 880–888.
Tsong, T.Y., 1989. Electroporation of cell membranes. In: Electroporation and Electrofusion in Cell Biology. Springer.
Weiss, N.G., Jones, P.V., Mahanti, P., Chen, K.P., Taylor, T.J., Hayes, M.A., 2011. Dielectrophoretic mobility determination in DC insulator-based dielectrophoresis. Electrophoresis 32, 2292–2297.
Wen, J., Tan, X., Hu, Y., Guo, Q., Hong, X., 2017. Filtration and electrochemical disinfection performance of PAN/PANI/AgNWs-CC composite nanofiber membrane. Environ. Sci. Technol. 51, 6395–6403.
Zhou, J., Wang, T., Xie, X., 2019. Rationally designed tubular coaxial-electrode copper ionization cells (CECICs) harnessing non-uniform electric field for efficient water disinfection. Environ. Int. 128, 30–36.